Available online at www.sciencedirect.com
ScienceDirect
Trans. Nonferrous Met. Soc. China 27(2017) 1517−1529
Transactions of Nonferrous Metals Society of China
www.tnmsc.cn

Scope for improved properties of dissimilar joints of ferrous and non-ferrous metals

Gopinath THIRUNAVUKARASU, Subrata CHATTERJEE, Sukumar KUNDU

Department of Metallurgy and Materials Engineering,
Indian Institute of Engineering Science and Technology, Shibpur, Howrah 711103, India

Received 31 May 2016; accepted 4 October 2016

Abstract: Dissimilar joints (DSJs) of ferrous and non-ferrous metals have huge technological importance in the frontiers of new designs in new machineries and improved design of conventional systems. This investigation was undertaken to improve mechanical properties of joints of two dissimilar metals: one is Ti-based and the other is Fe-based. DSJs were processed using bonding pressure from 1 to 9 MPa in step of 2 MPa at 750 °C for 60 min. Properties of the DSJs of these two metals using different mechanisms and methods were compared with the present research for verification. Experimental results from the diffusion bonding mechanism for joining the dissimilar metals validated the improvement in properties. Superior mechanical properties of dissimilar-metals joints were achieved mainly due to the third non-ferrous metallic foil, Ni of ~ 200-μm thickness, which avoided the formation of brittle Fe−Ti-based intermetallics in the diffusion zone. DSJs processed are able to achieve maximum strength of ~560 MPa along with substantial ductility of ~11.9%, which is the best ever reported in the literatures so far. Work hardening effect was detected in the DSJs when the bonding was processed at 5 MPa and above. Bulging ratio of the non-ferrous metal (Ti-based) was much higher than that of the ferrous metal (SS) of the DSJs processed. SEM analysis was carried out to know the details of reaction zone, while XRD was carried out to support the SEM results. Reasons for change in mechanical, physical, and fracture properties of the DSJs with the process parameter variations were clarified.

Key words: diffusion welding; titanium alloy; stainless steel; nickel; interlayer; tensile strength; fractograph

1 Introduction

Among the manufacturing technologies known to the human race, joining is acknowledged as a key technology with innovativeness in design, flexibility and productivity in processing, and easiness in maintaining or repairing. Although the concept of additive manufacturing (as opposed to subtractive manufacturing techniques, such as traditional machining) is gaining its momentum of application in creating new products every day from the start of the 21st century, engineers and scientists deemed the notion to produce ‘‘joint-free’’ products with competitive functions and cheaper price is favorably unrealistic in most cases. Hence, to reap the benefits of different materials properties, the design of hybrid structures demands the presence of joints of dissimilar materials. Several industries such as aeronautics, automotive, clothing, marine application, mechanical tooling, medical implants, nuclear, power generation, sports goods, satellites and space-vehicles achieved the improved product performance due to the joints of dissimilar materials in multi-material hybrid structures [1].

Fusion welding is one of the most widely used methods for the joining of metals. Fusion welding of the dissimilar-metal combinations is quite difficult. These difficulties include problems associated with metallurgical incompatibility, e.g., the formation of brittle phases, the segregation of high- and low-melting phases due to chemical mismatch, and possibly large residual stresses from the physical mismatch. In addition to fusion welding, several other types of joining techniques are also available, and may often be associated with less difficulty for producing dissimilar-metal joints. Survey on the processes used for producing dissimilar-metal joints showed clearly that diffusion bonding (DB) is the most frequently investigated process in the joining of dissimilar metals [2].

Dissimilar joints (DSJs) of ferrous and non-ferrous metals are much more interesting in the view point of application and much more challenging in the view point

Corresponding author: Sukumar KUNDU; Tel: +91-033-26684561-63; Fax: +91-033-26682916; E-mail: skundu@metal.iiests.ac.in
DOI: 10.1016/S1003-6326(17)60172-9

of research. Many researchers undertook the experimental investigations to realize the DSJs of ferrous and non-ferrous using different techniques. SHANMUGARAJAN and PADMANABHAM [3] carried out investigations on laser welding (LW) on the titanium (Ti) and stainless steel (SS) combination. They observed that both autogenous welds of Ti/SS and the welds using V as interlayer have exhibited extensive cracking; however, DSJs with Ta as interlayer could achieve the maximum strength of ~40 MPa. HE et al [4] studied the effect of processing parameters on the diffusion bonded DSJs of Ti-alloy and SS directly and with a Ni interlayer. The maximum shear strengths of the joints achieved were ~72 MPa and ~148 MPa for direct bonding and indirect bonding using Ni interlayer, respectively. The optimum parameters for DB were temperature of 850−880 °C, specific stress of 10−15 MPa, and bonding time of 10−20 min. They showed improvement in the performance of the joints by ~100% by using Ni interlayer. EROĞLU et al [5] used DB technique to join Ti−6Al−4V alloy to microduplex SS using a pure Cu interlayer (~20 μm). The maximum shear strength of ~107 MPa was achieved for the joints processed under 0.2 MPa at 900 °C for 5 min. In their study, it was observed that FeTi intermetallic is more deleterious than $CuTi_2$. They proposed that a high heating rate and a short holding time must be used in the DB of Ti−6Al−4V to microduplex SS when pure Cu interlayers were used.

ELREFAEY and TILLMANN [6] evaluated vacuum brazed cp-Ti and low-carbon steel joints using Cu-based alloy and two Ag-based braze alloys. The maximum strength of ~113 MPa was achieved for the specimen brazed at 750 °C using Ag−27.25Cu−12.5In−1.25Ti filler alloy. ÖZDEMIR and BILGIN [7] investigated properties of diffusion bonded Ti−6Al−4V to AISI 304 stainless steel with Cu interlayer. Bonding was carried out at temperatures of 830, 850, and 870 °C for holding time of 50, 70, and 90 min, respectively, under 1-MPa load in argon atmosphere. The joints processed under 1-MPa load at 870 °C for 90 min of holding time gave the maximum strength of ~118 MPa. BALASUBRAMANIAN [8] achieved bonding strength of ~149 MPa for the DSJs of Ti−6Al−4V and 304 SS with adequate ductility using Ag as an interlayer through DB technique. The optimal strength was achieved for the joints processed under 5 MPa (bonding pressure), at 800 °C (bonding temperature) for 60 min (bonding time). BALASUBRAMANIAN [9] fabricated DSJs of Ti−6Al−4V and AISI 304 SS with Ag as interlayer. He claimed that successful bonding of the dissimilar metals was possible in the temperature range of 750−800 °C. Above 825 °C, bonding is not successful for this combination of dissimilar materials with Ag interlayer. The maximum lap shear strength of ~158 MPa was achieved under a bonding pressure of 5 MPa at 800 °C for 90 min. HE et al [10] investigated hot pressing and diffusion welding (HP−DW) of titanium alloy (TC4) to stainless steel (1Cr18Ni9Ti) with an Al-alloy (LF6) interlayer. The optimal tensile strength of ~183 MPa was achieved for the joints processed at 450 °C. Tensile samples failed at the SS/LF6 interface irrespective of the processing temperature chosen. The effect of LF6/TC4 interface on the properties of bonded joint is less than that of SS/LF6 interface.

THIRUNAVUKARASU et al [11] achieved the maximum strength of ~206 MPa for the diffusion bonded joints (DSJs) of Ti6Al4V/Ni/SS processed using 3 MPa at 750 °C for 60 min. They demonstrated that failure of the joints was initiated and propagated apparently at the TiA/Ni interface. ZAKIPOUR et al [12] made joints of dissimilar alloys 316L SS and Ti−6Al−4V using transient liquid phase (TLP) bonding mechanism. The effect of Cu interlayer with different thicknesses on the properties of the joints was studied. The maximum shear strength of ~220 MPa was attained for the bond made at 900 °C using ~50-μm thick Cu interlayer. The decrease in shear strength of the bonds occurred due to the increase in width of joint zone and formation of Fe_2Ti brittle intermetallics at the interface. SHIUE et al [13] advocated using (Ni)/Cr barrier layers in brazing Ti−6Al−4V and 17-4PH SS. They achieved the maximum strength of ~233 MPa. VIGRAMAN et al [14] studied the microstructure and tensile properties of DBJs between Ti−6Al−4V and AISI 304L using the pressures of 4 MPa and 8 MPa in the temperature range of 875−950 °C for 60 min. They achieved the maximum strength of ~242 MPa for joints processed using 4 MPa at 900 °C for 60 min and annealed for 2 h at 750 °C. KATO et al [15] were one group of the leading groups worked in synthesizing joints of dissimilar metals of ferrous and non-ferrous types in the early periods using diffusion welding (DW) technique. They joined Ti and SS rods by DW under phase transformation in air. Ti/SS assemblies were heated to above the transformation temperature of Ti and cooled below that temperature one, two, or three times by alternately applying and breaking an electric current. Ti/SS joints were bonded using bonding pressure of 15.8 MPa in thermal cycle range of 677−1000 °C with the maximum of 3 cycles. The welding process was finished within few minutes. In Ti/SS welds, a joint interface was observed inside the specimen, but there was no gross void at the interface. The maximum tensile strength of ~260 MPa was achieved by the Ti/SS joints in their study. KURT et al [16] carried out investigation on the effects of bonding temperatures on the properties of diffusion bonds between Ti−6Al−4V alloy and AISI 316L SS.

Intermetallic phases such as FeTi and Fe_2Ti were observed at the interfaces. The highest shear strength of ~270 MPa was obtained for diffusion bonds processed under a pressure of 5 MPa at 885 °C for 30 min. GHOSH and CHATTERJEE [17] studied direct DB of Ti−6Al−4V to 304L SS in vacuum in the temperature range of 850−950 °C using 3 MPa uniaxial load for 30−90 min. XRD and SEM−EDS analysis indicated the presence of Fe−Ti-based intermetallic phases at different locations in the reaction zone. The maximum strength of ~295 MPa was obtained for the joint processed at 850 °C for 60 min. FENG et al [18] made DSJs of TiAl and steel using Ag−Cu−Ti filler metal. The joints achieved the best strength of ~298 MPa when brazed at 870 °C for 15 min.

SHENG et al [19] carried out solid-state DB of Ti-alloy to austenitic stainless steel without interlayer. The test results showed that the ultimate tensile strength of the joint reached its maximum value (~307 MPa) when processed under the bonding pressure of 5 MPa at the cyclic bonding temperature of T_{max}=890 °C and T_{min}=800 °C for bonding time of 120 s. TOMASHCHUK et al [20] studied the electron beam welds between Ti-alloy and AISI 316L SS with a Cu foil. Beam shift toward the Ti-alloy side resulted in large amount of brittle Fe_2Ti phase whereas beam shift toward the steel side inhibited the formation of brittle intermetallics at interface. The maximum tensile strength of ~350 MPa was achieved by the DSJs. THIRUNAVUKARASU et al [21] studied the DSJs of Ti−6Al−4V (TiA) and 304 stainless steel (SS) using pure nickel (Ni) as an intermediate material. The maximum tensile strength of ~382 MPa was observed for the joints processed using 4 MPa at 750 °C for 60 min. It was reported that the extent of diffusion zone at Ni/SS interface was greater than that of TiA/Ni interface.

DEY et al [22] attempted friction welding (FW) of Ti to 304L SS. FW parameters were optimized to produce joints that are stronger. They welded joints with 100 MPa friction pressure and achieved the maximum strength of ~400 MPa. They pointed out the application of the joint in nuclear industry where the dissolution of spent fuel was carried out in a vessel (made of Ti) and the dissolved solution was transported through the 304L SS pipes. LEE and JUNG [23] investigated the microstructures and mechanical properties of the friction welded Ti/SS. Joints processed with high upset pressure of ~400 MPa and friction time of ~0.5 s yielded the maximum strength of ~420 MPa. They proposed that higher mechanical properties were acquired under higher upset pressure condition due to higher compressive force between bonded materials, smaller grain size and narrower thickness of reaction layer. KUMAR and BALASUBRAMANIAN [24] friction welded Ti−6Al−4V and SS 304L. They reported sound welding zone of the dissimilar metals but the joints were not successful during drop test due to the crack formation and the brittle intermetallic compound in the weld zone. They introduced Cu interlayer which improved the strength of the friction-welded dissimilar-metals joints in the order of ~523 MPa.

In this work, chemistry of interfacial reaction zones and physics along with mechanical properties of dissimilar metal joints of 304 stainless steel (ferrous) and Ti−6Al−4V (non-ferrous) using Ni (non-ferrous diffusion-aid metal layer) were focused. DSJs were synthesized using diffusion bonding (DB) technique. DB is a high-temperature solid-state welding process that permanently joins mating surfaces by simultaneous application of pressure and heat. It does not involve macroscopic deformation, melting, or relative motion of the parts welded. A solid filler metal (diffusion aid) may be inserted between the faying surfaces [25]. DB has demonstrated its uniqueness by finding application in the processes and products of front line areas of science and technology. DB is actually gaining its momentum of applicability from the days of conception due to the inappropriateness of other joining techniques. The main factors which influence DB process are bonding pressure, temperature, and time [26]. Literatures are plenty to know the details of influence of bonding temperature or bonding time on the DBJs of dissimilar metals, but the knowledge of influence of bonding pressure on the properties of DBJs is scanty. This research was dedicated to know the evolution of interfacial microstructure and mechanical properties of DSJs of ferrous metal (304 SS) and non-ferrous metal (Ti−6Al−4V) using a non-ferrous diffusion-aid (Ni) metallic layer of ~200-μm thickness due to variation in the bonding pressure parameter.

2 Experimental

2.1 Parent metals and third metal preparation

Ti−6Al−4V (mass fraction, %) (TA), 99.5% Ni (mass fraction) ((200±10) μm), and Fe−18Cr−8Ni (mass fraction, %) (SS) were used in this investigation. Room-temperature mechanical properties of the base metals (TA and SS) were presented in Table 1. Parent metals were of cylindrical shape with diameter of ~15 mm. DB experiments were carried out on samples of two different sizes. Interfacial analysis, microhardness evaluation, and diffraction study were carried out on sample with 7 mm in length (referred: optical sample), whereas the tensile testing was carried out with 30 mm long sample (referred: tensile sample). Before bonding, mating surfaces of base metals and foil were ground using series of SiC emery papers (from 40 to 1600 grit) to improve the quality of surface roughness followed by final polishing using 1-μm diamond paste to get scratch-

free surface and followed by cleaning with C_2H_5OH. Ni was thinned down from 260 to (200±10) μm. Surface roughness of the faying surfaces was measured using Mitutoyo surface roughness tester (SJ−301). Surface roughness (R_a) of mating surfaces was measured to be ~0.02 μm. Parent metals and interlayer were ultrasonically cleaned in acetone for 120 s. Ni was then sandwiched between TA and SS.

Table 1 Room-temperature mechanical properties of base metals

Alloy	$\sigma_{0.2}$/ MPa	Ultimate tensile strength/MPa	Fracture elongation/ %	Microhardness (HV)
TA	886.3±9	978.0±11	20±0.2	400
SS	699±10	782.5±9	44±0.3	300

2.2 Diffusion welding machine and DSJs preparation

TA/200-μm-Ni/SS assemblies were kept on fixed supporting pedestal of the indigenously-made welding fixture (Fig. 1). The bonding pressure was applied along the longitudinal direction of the sample. Uniaxial compressive load was applied from top by means of hand-driven screw-type shaft. The joining operation was carried out using pre-decided bonding pressure (bonding pressures ranging from 1 to 9 MPa in step of 2 MPa). Welding fixture with the assemblies was inserted into a vacuum chamber (Fig. 2) equipped with two stages of vacuum pump. Initially, vacuum was created using single-stage rotary vacuum-pump and the oil-vapor diffusion-pump was used to improve the fineness of the vacuum. After attaining the required vacuum ((6−8) × 10^{-3} Pa), temperature was increased from room temperature (30 °C) to 750 °C (bonding temperature) at the rate of 0.24 K/s. DB experiments were conducted in electrical resistance heating, using nichrome wire, split-type cylindrical furnace with constant temperature zone of 50 mm (diameter), and controlling the temperature within ±4 °C with the capability of operating even at 1000 °C. Temperatures at the interfaces of the DB sample were monitored using chromel−alumel thermocouple kept ~2.5 mm away from the joint interface. The TA/200-μm-Ni/SS assemblies were held for 60 min (bonding time interval) in vacuum at 750 °C (bonding temperature). After 60 min of holding at 750 °C, the assemblies (TA/200-μm-Ni/SS) were converted to TA/200-μm-Ni/SS DSJs. After the experiment was completed, diffusion-bonded samples were furnace-cooled to 150 °C at a cooling rate of 0.09 K/s in vacuum. To avoid the overheating while operating, the DB chamber and the oil-vapor diffusion-pump chamber were continuously cooled using a water-circulation system. The images of the diffusion welded optical sample and tensile sample are given in Fig. 3.

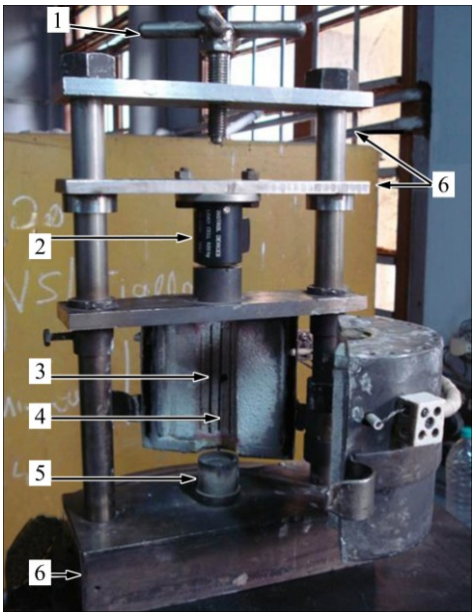

Fig. 1 Details of indigenously designed and manufactured welding fixture (1—Threaded shaft for applying pressure; 2—Pressure sensor (Max: 500 kg load); 3 — Thermocouple (Chromel−alumel); 4—Heating element (Nichrome material); 5—Fixed pedestal (Molybdenum material) for supporting to-be welded samples; 6—Frame (304 SS material))

Fig. 2 Vacuum chamber surrounded by copper tubes for water circulation provision

2.3 Characterization of DSJs

2.3.1 Interfacial microstructure and diffractometric study of DSJs

The optical sample (Fig. 3) of DSJs was sectioned transversely to the bond interface, then ground followed by diamond polishing. Polished surfaces (Fig. 4) of

optical samples of DSJs were examined by a scanning electron microscope (JSM−5510, JEOL) in back-scattered electron (SEM−BSE) mode to obtain finer structural details of the diffusion zone at the interfaces. Chemical composition (in mole fraction, %) of the reaction layers was determined by energy dispersive spectroscopy (SEM–EDS, Thermo Electron Corporation, Noran System Six C10018) using SiLi detector. Intermetallics were predicted using the above chemical analysis and Ni−Ti phase diagram. The existence of these intermetallics was confirmed by X-ray diffraction (XRD) study on the fracture surfaces of the DSJs. XRD analysis (Philips PW 1830) was carried out using Co as target at an operating voltage of 35 kV with sample current of 25 mA. Scanning range (2θ) from 30° to 110° with a step size of 0.01°(2θ) was used.

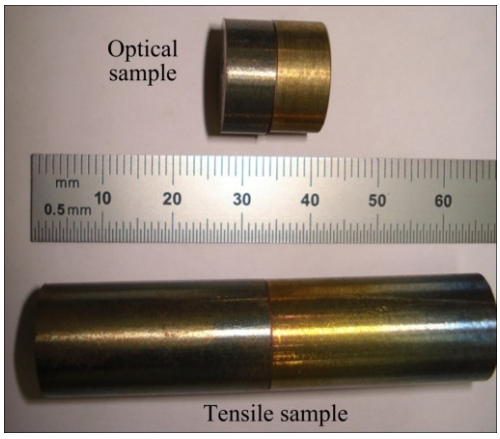

Fig. 3 Typical diffusion bonded optical sample and tensile sample of dissimilar metal joints of TA and SS

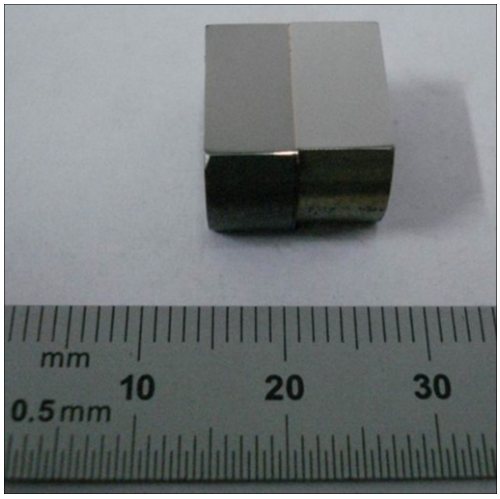

Fig. 4 Typical polished (unetched) optical sample of DSJs of TA and SS

2.3.2 Mechanical properties of DSJs

Both ferrous and non-ferrous metals which were diffusion bonded underwent some changes in shape. Whenever a force is applied to a solid object, a stress is produced within the object. The physical effect/ manifestation of this stress is that the object experiences some amount of deformation, a strain. Hence, it was decided to calculate the bulging ratio of the DSJs. Bulging ratio α_{BR} [15] of the DSJs is defined as follows:

$$\alpha_{BR}=(d_1-d_0)/d_0\times100\% \quad (1)$$

where d_1 and d_0 are the diameters of the ferrous/non-ferrous metals at the joint interface after and before welding experiment, respectively.

Mechanical properties (at room temperature) of transition joints were evaluated by tensile and hardness tests. The tensile strength and the respective ductility were evaluated on Instron 4204 at a crosshead speed of 8.33×10^{-4} mm/s. Cylinder-shaped tensile specimens (Fig. 5) were machined as per ASTM specification E8M−11 with gauge diameter and length of 4 and 20 mm, respectively [27]. Metallic foil was almost kept at the centre of gauge length of the tensile sample. The average of the three samples tested at each bonding pressure was reported here.

Fig. 5 Typical tensile specimens machined out of tensile sample of DSJs of TA and SS

Microhardness measurements were carried out on the polished surface of optical samples (Fig. 4) at different points across the base-metal/interlayer/base-metal using the microhardness tester (Leica VMHT) and Vickers diamond indenter with a load of 0.25 N for dwelling time of 20 s. To measure microhardness across the interfaces of the DSJs, the whole area of the polished surface (Fig. 4) was divided from one-end of the base-metal to the other end of the base-metal by successive planes separated by 10-μm interval, then five successive indentations were made on a particular

section at different locations, the average value was reported here for concise representation of the data. Microindendation on a section was carried out in different zones so that the interaction between the successive indentations was minimized to the utmost possible extent.

2.3.3 Fracture surface and fracture path of DSJs

DSJs were fractured under tensile loading. Fracture surfaces of tensile fractured DSJs were observed in secondary electron mode of SEM (JSM−5510, JEOL) using energy dispersive spectroscopy (Thermo Electron Corporation, Noran System Six C10018) to reveal the distinguishable features and to understand the nature of the failure of DSJs during tensile testing. To observe the fracture path, the authors prepared conductive mounts (using copper filler) of the TA and SS sides of the tensile-tested DSJs. SEM−BSE observations were also made on the conductive mounts prepared to ascertain the particular site of fracture path in order to know the most likely locations apparently through which the failure was initiated and propagated during tensile testing.

3 Results and discussion

3.1 Interfacial microstructure of DSJs

The understanding of influence of bonding pressure on the mechanical properties of DSJs is incomplete and erroneous from the point of view of physical metallurgy of the DSJs of dissimilar-metals using metallic-layer because the scientific investigation was primarily interested in correlating the microstructure with mechanical properties for broadening the spectrum of applications of the joints from very simple engineering problems to the cutting-edge technologies. The requirement for low order magnification SEM−BSE images (Fig. 6) was: firstly (qualitative), it could facilitate the comparison of the profiles at both the interfaces (TA/Ni and Ni/SS) in a DSJ (processed at a particular bonding pressure) and between DSJs (processed at different bonding pressures); secondly (quantitative), the extent of diffusivity could be measured by measuring the distance between the interfaces (TA/Ni and Ni/SS); and thirdly (qualitative), the quality of the bond could be ascertained with the details of discontinuity and voids at the interfaces. The absence of discontinuity and voids at both interfaces was revealed, which established the superior contact of the mating surfaces with process parameters. Hence, DSJs were efficacious. The profile of the interfaces (both TA/Ni and Ni/SS) was planar in nature regardless of the selected bonding pressure, which demonstrated that the interfacial interactions were in steady state. The lower magnification SEM–BSE images (Fig. 6) did not provide the inherent latent details of the interfacial reactions; hence, SEM–BSE images at higher order magnification at TA/Ni interface (Fig. 7) and Ni/SS interface (Fig. 8) were required for better understanding. The SEM–BSE images (Fig. 8) of Ni/SS interface of the DSJs revealed solid solution behavior. Layer wise intermetallics were observed at the TA/Ni interface (Fig. 7) of the DSJs.

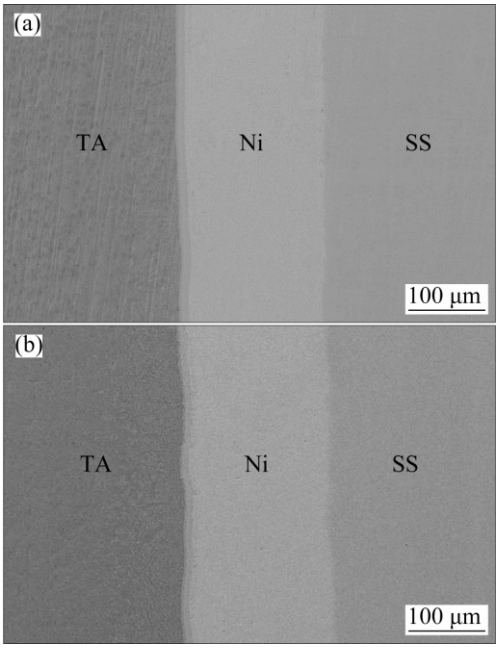

Fig. 6 SEM–BSE images of DSJs processed at 1 MPa (a) and 9 MPa (b)

It was observed from Fig. 7 that the TA/Ni interfaces of the DSJs processed using 3, 5, and 7 MPa had only one light shaded reaction layer consisting of Ti (~27%, mole fraction) and Ni (~70%, mole fraction). Hence, the Ni−Ti phase diagram indicated the realization of Ni_3Ti intermetallic [28,29]. The TA/Ni interface of the DSJs processed using 1 and 9 MPa had two successive reaction layers. The deep shaded reaction layer observed adjacent to the TA matrix consisted of Ti (~50%, mole fraction) and Ni (~45%, mole fraction). Hence, the Ni−Ti phase diagram indicated the possibility of realization of NiTi intermetallic [28,29]. The reaction layer adjacent to the Ni matrix was light shaded Ni_3Ti intermetallic. In general, for all DSJs the width of Ni_3Ti intermetallic was wider compared to that of the NiTi intermetallic in the reaction zone [11,21]. The similar Ni–Ti-based reaction products were also observed in Refs. [30,31]. Sensible reasons for the presence of the layer-wise Ni−Ti-based intermetallics at the TA/Ni interface and the solid−solution behavior at the Ni/SS interface could be comfortably explained using Hume-Rothery rules and the principle of electronegativity [11,21]. At the interface, the atoms from both the sides diffuse in the opposite direction, but there is an effective diffusion of atoms at each interface which is more predominant than that in the

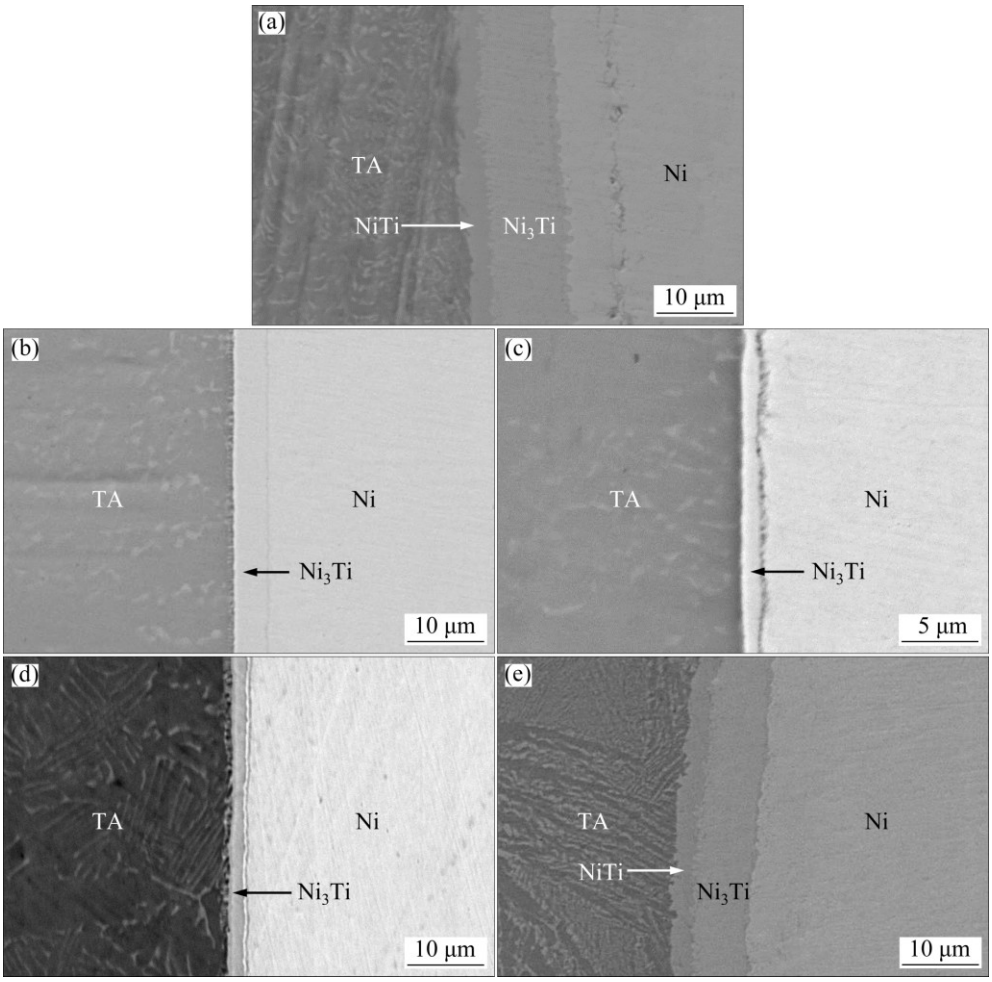

Fig. 7 SEM−BSE images of TA/Ni interface of DSJs processed at 1 MPa (a), 3 MPa (b), 5 MPa (c), 7 MPa (d), and 9 MPa (e)

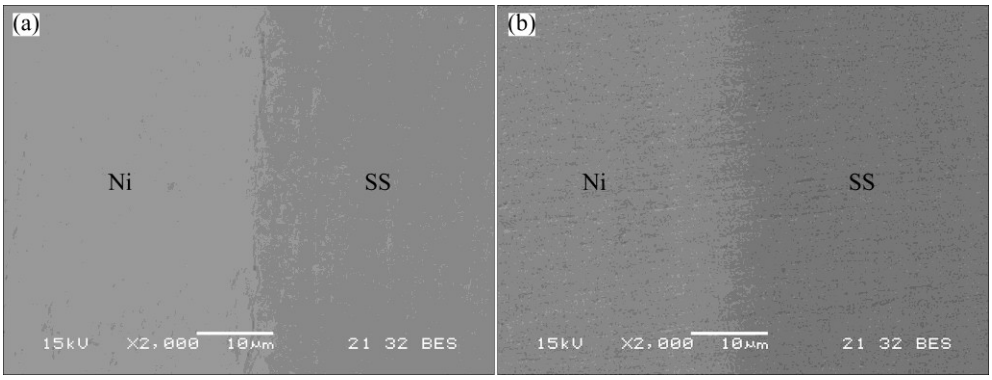

Fig. 8 SEM−BSE images of Ni/SS interface of DSJs processed at 1 MPa (a) and 9 MPa (b)

other direction. At the TA/Ni interface, Ni atoms could diffuse further deeply into TA matrix as compared to the diffusing capability of Ti atoms into Ni matrix; whereas net flux of Ni atoms past the interface in one direction was faster than the flux of atoms in SS in the opposite direction. Hence, the effect proposed by Kirkendall was observed at Ni/SS interface for all the DSJs [11,21].

With increase in the bonding pressure from 1 to 5 MPa, reaction zone width at the TA/Ni interface (Fig. 7) decreased. Decrease in the reaction zone width is due to the decrease in the net-activity of atoms at the interfaces. Most of our engineering materials are polycrystalline so that the grain boundary diffusion is far more important than surface diffusion. Deformation forces the dislocations that exist in a polycrystalline metal to move up, and pile up at the grain boundaries, and new dislocations to be generated. Consequently, the increase in pressure hinders the grain boundary diffusion which

affects the surface diffusion phenomenon; and hence, the interfacial activity was affected [32−34]. Diffusion along the free surfaces is a dominant diffusion path. A free surface is associated with more open structures and experiments showed that the jump frequency for atoms diffusing along this defect is higher than that for diffusion in lattice and grain boundaries. With the increase in bonding pressure from 5 to 9 MPa, the effective free surface for contact of the mating surfaces was increased, thus the atomic mobility increased across the interface; hence, the reaction zone width at TA/Ni interface increased.

3.2 XRD analysis of DSJs

The XRD patterns (Fig. 9(a)) showed representative peaks of α-Ti, β-Ti, NiTi, Ni_3Ti and Ni. XRD pattern (Fig. 9(b)) of the fractured surfaces along SS side showed representative peak of γ-Fe, Ni and Ni_3Ti. The presence of NiTi intermetallic observed through XRD on TA side of the DSJs processed using 5 MPa was not proven through SEM−BSE studies presumably due to its low volume fraction. The presence of other phases except NiTi observed through XRD, on both TA and SS sides, was well identified through respective SEM−BSE studies. From the XRD analysis, it was observed that there exists quite significant evidence that the DSJs were most likely fractured along TA/Ni interface. THIRUNAVUKARASU et al [11,21] showed that DSJs failed at the TA/Ni interface.

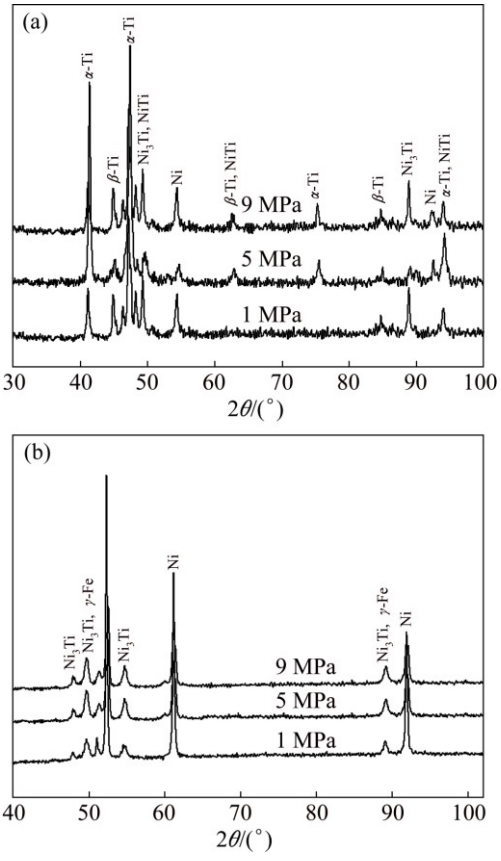

Fig. 9 XRD patterns of fracture surfaces of TA side (a) and SS side (b) of DSJs processed using different bonding pressures

3.3 Surface property of DSJs

It was observed that the hardness of the non-ferrous metal side (TA) (Fig. 10) of the DSJs was HV ~400 irrespective of the bonding pressure adopted during experiments. The hardness of the ferrous metal side (SS) witnessed to be HV ~300 for the DSJs processed below 5 MPa, whereas the surface hardness of SS side was HV ~400 for the DSJs processed at 5 MPa and above.

In the same way, the hardness of the interlayer zone (Ni) of the DSJs was found to be HV ~175 for the DSJs processed below 5 MPa, whereas HV ~200 for the joints processed at 5 MPa and above. It was observed that the increase in the bonding pressure had a significant influence on increasing the surface property (hardness) of SS side and Ni zone, but such phenomenon was not observed on TA side.

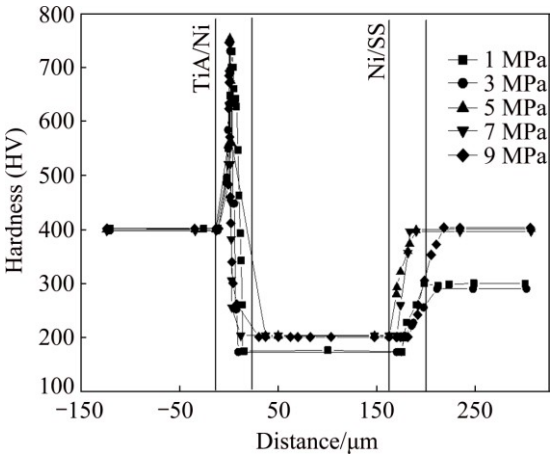

Fig. 10 Microhardness profile along interfaces of DSJs processed using various bonding pressures

The increase in the hardness of the Ni and SS with the increase in pressure could be attributed to the effect of work hardening. When material is deformed, the work hardening occurs, resulting in the increase of the hardness of the material. In general, the rate of work hardening is lower for HCP metals than that for cubic metals. TA is HCP metal whereas Ni and SS are cubic metals. The hardness values of Ni and SS were increased significantly with the increase in the bonding pressure from 3 to 5 MPa and above, while the hardness of TA (HCP metal) does not change with the increase of the bonding pressure [35,36].

Along Ni/SS interface, hardness increased from Ni to SS and the observed hardness was HV ~220 for the DSJs processed using bonding pressure below 5 MPa, whereas HV ~330 for 5 MPa and above. Along the TA/Ni diffusion zone, the hardness increased initially till

it reached the maximum value and then dropped towards Ni. The hardness values of NiTi intermetallic and Ni_3Ti intermetallic were HV ~550 and HV ~750, respectively. The hardness at NiTi/Ni_3Ti interface was HV ~650. It was also noticed that the fracture was expected to occur apparently near the TA/Ni interface because the hardness of TA/Ni interface (HV ~750) was much greater than that of Ni/SS interface (HV ~330), thus the TA/Ni interface was more brittle as compared to the Ni/SS interface. SAM et al [37] demonstrated that DSJs failed through the TA/Ni-alloy interface.

3.4 Bulging property of DSJs

The bulging ratio (Fig. 11) of non-ferrous metal (TA) of the DSJs was much higher than that of the ferrous metal (SS) of the respective DSJs. The reason for the significant differences in the bulging ratios of TA side and SS side needs to be addressed. Here, the bulging (lateral deformation) of the metals welded was of inelastic-type (precisely, plastic deformation); however, the plastic deformation of materials can be correlated with the elastic properties of the respective materials. There are three elastic moduli which derive from the spatial tri-dimensionality of the world. The three elastic moduli represent linear, planar, and volume effects on material. Apart from these elastic moduli, there is another property called Poisson ratio (μ) defined as the ratio of the transverse to the axial strain. These elastic moduli are generally anisotropic in the case of single crystal but the assumption of isotropic is valid for polycrystalline materials in which the individual crystallites are arranged completely random [38−40]. Although change in volume is related with the bulk modulus (K) of the material it can be related with the other elastic moduli using the following relationships (Eqs. (2) and (3)) [40]:

$$E=3K(1-2\mu) \tag{2}$$

$$E=2G(1+\mu) \tag{3}$$

Using Eqs. (2) and (3), it could be perceived that the elastic modulus (E) of materials could be able to explain the potential causes for significant differences in the bulging ratios of TA side and SS side of the DSJs. The elastic moduli of Ti-alloy (Ti−6Al−4V) and austenitic stainless steels (304 SS) are ~110−130 GPa [41] and ~190−206 GPa [42], respectively. As the elastic modulus of Ti−6Al−4V is much lower as compared to the elastic modulus of 304 SS, the non-ferrous metal (TA) side of the DSJs underwent an excess amount of bulging as compared to ferrous metal (SS) side of the respective DSJs. Hence, it could be stated that the bulging ratio (α_{BR}) of the material is inversely proportional to its elastic modulus (E) (Eq. (4)).

$$\alpha_{BR} \propto 1/E \tag{4}$$

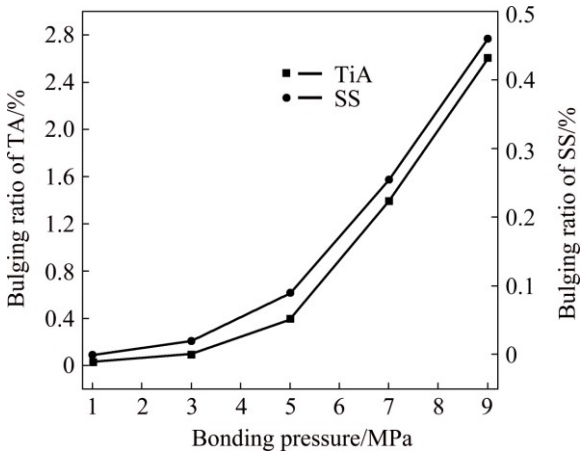

Fig. 11 Variation of bulging ratios of TA and SS of DSJs with respect to bonding pressure applied

It was also observed from the bulging ratio graph (Fig. 11) that the slope of the bulging ratio increased with the bonding pressure applied. Mathematically, the slope of the bulging ratio was in increasing order (Eq. (5)) with the bonding pressure utilized. Hence, the lower-range has less slope than the middle-range, and the middle-range has less slope than the higher-range of bonding pressure (p).

$$p \propto \alpha_{BR} \tag{5}$$

3.5 Tensile properties of DSJs

With the increase in the bonding pressure from 1 to 5 MPa, both tensile strength and ductility of the DSJs increased steeply. With the increase in bonding pressure from 1 to 5 MPa, the coalescence of the mating surfaces of the DSJs was improved. Hence, the improvement in the tensile properties of the DSJs was favored. The DSJs did not show much increase in its tensile strength beyond the bonding pressure of 5 MPa, although the ductility of the DSJs dropped infinitesimally. DSJs processed using 5 MPa achieved the maximum strength of ~560 MPa along with substantial ductility of ~11.9%. From the tensile properties of the DSJs (Fig. 12), it was ascertained that bonding pressure less than 5 MPa has significant influence on the tensile properties of the DSJs, whereas the application of bonding pressure beyond 5 MPa does not contribute much to improving the strength property of joints of dissimilar metals. Hence, it could be said comfortably that bonding pressure of 5 MPa is the optimal level of the input parameter to maximize the strength behavior of the joints of ferrous and non-ferrous metals. Increase in the bonding pressure improved the interfacial contact area between the mating surfaces of the diffusion bonds; however, work hardening effect [43] on the assemblies of the DSJs was observed for the joints processed at 5 MPa and above bonding pressures. The maximum strength (~560 MPa)

achieved in this study is the best performance of DSJs of Ti−6Al−4V and SS till date reported using different joining mechanisms (EBW, FSW, LW and TLP) in Refs. [3−24]. Hence, diffusion welding proved itself to have the time-tested technique for achieving improved properties of the DSJs of ferrous and non-ferrous metals using a third metal layer of non-ferrous type.

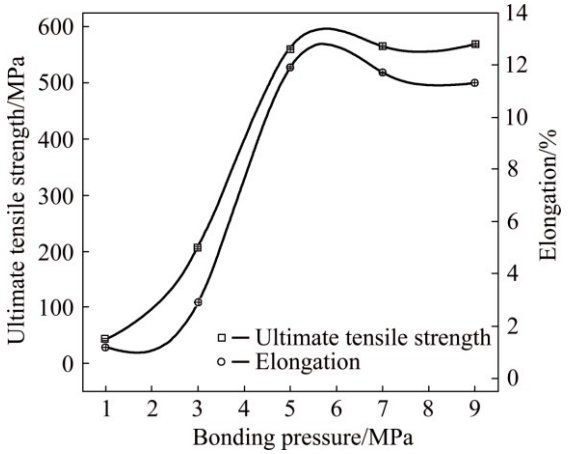

Fig. 12 Tensile properties of DSJs processed using various bonding pressures

3.6 Fracture surface analyses of DSJs

The fracture characteristics of TA side (Fig. 13(a)) and SS side (Fig. 13(b)) of DSJ processed using 1 MPa did not show any sign of neither dimpled-rupture (ductile) mode of failure nor the faceted river-pattern rupture (brittle) mode of failure. Most of the appearances in the fractograph of TA side (Fig. 13(a)) were visually featureless. Similarly, the appearances of SS side (Fig. 13(b)) were also featureless; additionally, cracks (white arrow marks in Fig. 13(b)) were visibly running throughout the fracture surface. It was wished to correlate the fractural observations of DSJs processed using 1 MPa with mechanical properties of the same. It was noted that the DSJs processed using 1 MPa were able to achieve strength of ~42.5 MPa. Poor strength of the DSJs processed using 1 MPa and featureless fracture surfaces indicated that the coalescence of the mating surfaces was incomplete due to the insufficient bonding pressure to create perfect interfacial bonding of the mating surfaces.

Both fracture geographies of TA side (Fig. 13(c)) and SS side (Fig. 13(d)) of DSJ processed using 9 MPa revealed two distinct regions. Hence, it could be comfortably claimed that the DSJs processed using 9 MPa had undergone mixed mode of failure. Firstly, the zones identified as white-circles (Figs. 13(c) and (d)) were faceted river-pattern rupture (brittle) mode of failure; secondly, the zones identified using black-rectangles (Figs. 13(c) and (d)) were dimpled-rupture (ductile) mode of failure of transgranular type. In general, it was learnt that the lowest bonding pressure (1 MPa) yielded featureless fractographs due to insufficient bonding; the increase in the bonding pressure to 9 MPa yielded the mixed mode fractural features.

3.7 Fracture path of DSJs

The fracture paths of the metallic mount sample prepared using tensile fractured DSJ processed at 7 MPa are shown in Fig. 14. The TA side (Fig. 14(a)) of the fractured joint did not show trace of Ni layer attached

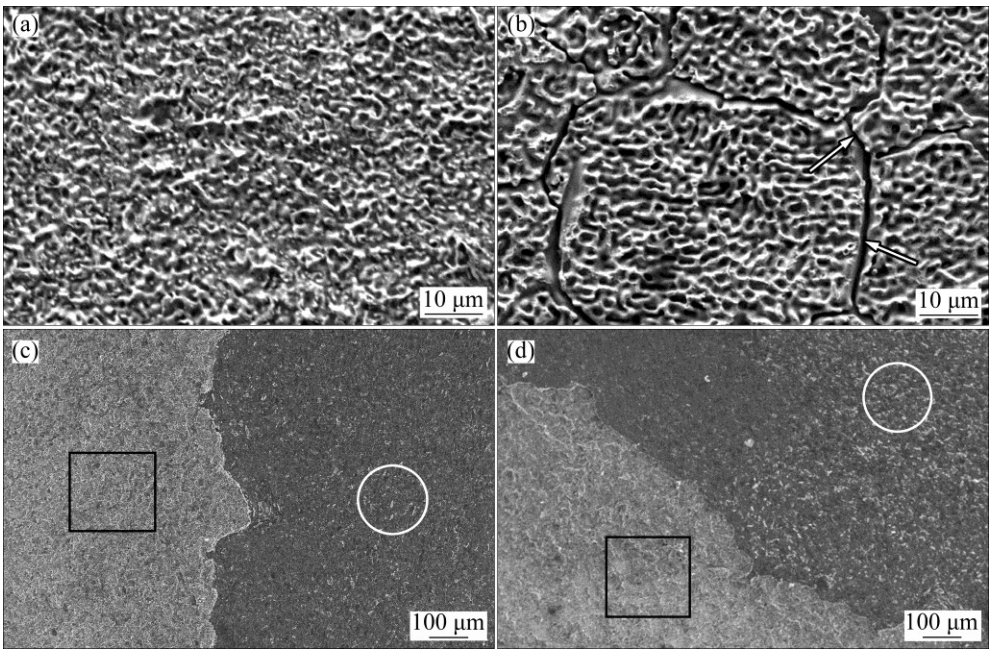

Fig. 13 Fracture surfaces of DSJs processed under different conditions: (a) 1 MPa, TA side; (b) 1 MPa, SS side; (c) 9 MPa, TA side; (d) 9 MPa, SS side

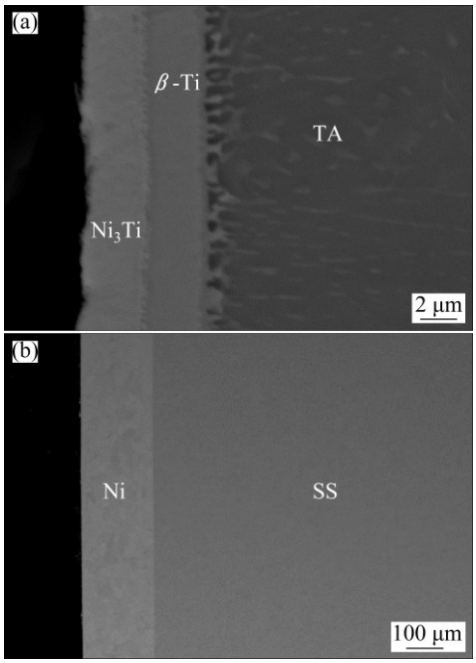

Fig. 14 Fracture paths of DSJs processed at 7 MPa: (a) TA side; (b) SS side

with, whereas the SS side (Fig. 14(b)) of the fractured joint revealed ample Ni interlayer. Hence, the SEM micrographs of the metallic mounts (Fig. 14) suggested that the TA/Ni/SS DSJs favored the fracture along the TA/Ni interface with the intermetallics (Ni_3Ti and NiTi) completely cleaved along the TA matrix.

In this study, the Ni/SS interface exhibited a perfect solid solution behavior irrespective of the bonding pressure selected. Hence, it could be claimed that the strength of the DSJs principally depend on the TA/Ni interface. And it was also noticed that the DSJ fractured at the TA/Ni interface, because the TA/Ni interface had higher hardness of HV ~750 as compared to the Ni/SS interface with the highest hardness value of HV ~330. Thus, the TA/Ni interface is more brittle as compared to the Ni/SS interface. It was noted that the hardness difference at TA/Ni interface (HV 550) was higher than that at Ni/SS interface (HV 200). Hence, the fracture propagated along the TA/Ni interface primarily due to the higher hardness difference as compared to the Ni/SS interface. This observation had attested the statement made by SIMÕES et al [44] that DSJs fractures at the interfaces with high hardness differences. The fracture path observation was quite consistent with the findings of the reported literatures [11,21,37] as well.

4 Conclusions

1) Bulging ratio of non-ferrous metal (TA) was much higher than that of the ferrous metal (SS) of the dissimilar joints (DSJs) processed. The significant difference in the bulging ratio of the base-metals (TA & SS) diffusion-bonded is explained using elastic modulus (E).

2) Work hardening effect was detected in the DSJs when the bonding was processed at 5 MPa and above bonding pressures.

3) DSJs processed at 5 MPa achieved maximum strength of ~560 MPa along with substantial ductility of ~11.9%. Tensile properties did not vary much when DSJs processed beyond 5 MPa. Considering the bulging ratio of the DSJs, 5 MPa was considered as the optimal welding pressure for achieving the best performance of the DSJs.

4) Using non-ferrous metallic-layer (Ni), deleterious Fe−Ti-based intermetallics in the diffusion zone was avoided. Hence, improved properties of the DSJs of ferrous–non-ferrous metals were achieved by using an appropriate non-ferrous metallic layer.

5) Diffusion welding has proved that it is the best available technique for achieving improved properties of dissimilar joints (DSJs) of ferrous and non-ferrous metals.

6) The fracture surfaces of DSJs processed at 1 MPa showed the featureless characteristic along with some cracks due to the insufficient bonding pressure to create perfect interfacial bonding of the mating surfaces. With the increase in bonding pressure to 9 MPa, mixed mode fractural features were prevalent.

7) Fracture path examination and surface property evaluation revealed that DSJs of TA/Ni/SS fractured along TA/Ni interface due to the higher hardness difference compared to the Ni/SS interface. Hence, TA/Ni interface is more brittle in nature than the Ni/SS interface.

References

[1] MARTINSEN K, HU S J, CARLSON B E. Joining of dissimilar materials [J]. CIRP Annals—Manufacturing Technology, 2015, 64: 679−699.

[2] SUN Z, KARPPI R. The application of electron beam welding for the joining of dissimilar metals: An overview [J]. Journal of Materials Processing Technology, 1996, 59: 257−267.

[3] SHANMUGARAJAN B, PADMANABHAM G. Fusion welding studies using laser on Ti−SS dissimilar combination [J]. Optics and Lasers in Engineering, 2012, 50: 1621−1627.

[4] HE P, ZHANG J H, LI X Q. Diffusion bonding of titanium alloy to stainless steel wire mesh [J]. Materials Science and Technology, 2001, 17: 1158−1162.

[5] EROĞLU M, KHAN T I, ORHAN N. Diffusion bonding between Ti−6Al−4V alloy and microduplex stainless steel with copper interlayer [J]. Materials Science and Technology, 2002, 18: 68−72.

[6] ELREFAEY A, TILLMANN W. Brazing of titanium to steel with different filler metals: Analysis and comparison [J]. Journal of Materials Science, 2010, 45: 4332−4338.

[7] ÖZDEMIR N, BILGIN B. Interfacial properties of diffusion bonded Ti−6Al−4V to AISI 304 stainless steel by inserting a Cu interlayer [J]. International Journal of Advanced Manufacturing Technology, 2009, 41: 519−526.

[8] BALASUBRAMANIAN M. Application of Box-Behnken design for fabrication of titanium alloy and 304 stainless steel joints with silver interlayer by diffusion bonding [J]. Materials and Design, 2015, 77: 161−169.

[9] BALASUBRAMANIAN M. Development of processing windows for diffusion bonding of Ti−6Al−4V titanium alloy and 304 stainless steel with silver as intermediate layer [J]. Transactions of Nonferrous Metals Society of China, 2015, 25: 2932−2938.

[10] HE P, YUE X, ZHANG J H. Hot pressing diffusion bonding of a titanium alloy to a stainless steel with an aluminum alloy interlayer [J]. Materials Science and Engineering A, 2008, 486: 171−176.

[11] THIRUNAVUKARASU G, KUNDU S, MISHRA B, CHATTERJEE S. Effect of bonding time on interfacial reaction and mechanical properties of diffusion-bonded joint between Ti−6Al−4V and 304 stainless steel using nickel as an intermediate material [J]. Metallurgical and Materials Transactions A, 2014, 45: 2067−2078.

[12] ZAKIPOUR S, HALVAEE A, AMADEH A A, SAMAVATIAN M, KHODABANDEH A. An investigation on microstructure evolution and mechanical properties during transient liquid phase bonding of stainless steel 316L to Ti−6Al−4V [J]. Journal of Alloys and Compounds, 2015, 626: 269−276.

[13] SHIUE R K, WU S K, SHIUE J Y. Infrared brazing of Ti−6Al−4V and 17-4 PH stainless steel with (Ni)/Cr barrier layer(s) [J]. Materials Science and Engineering A, 2008, 488: 186−194.

[14] VIGRAMAN T, RAVINDRAN D, NARAYANASAMY R. Effect of phase transformation and intermetallic compounds on the microstructure and tensile strength properties of diffusion-bonded joints between Ti−6Al−4V and AISI 304L [J]. Materials and Design, 2012, 36: 714−727.

[15] KATO H, SHIBATA M, YOSHIKAWA K. Diffusion welding of Ti/Ti and Ti/stainless steel rods under phase transformation in air [J]. Materials Science and Technology, 1986, 2: 405−409.

[16] KURT B, ORHAN N, KAYA M. Interface characterisation of diffusion bonded Ti−6Al−4V alloy and austenitic stainless steel couple [J]. Materials Science and Technology, 2009, 25: 556−560.

[17] GHOSH S K, CHATTERJEE S. On the direct diffusion bonding of titanium alloy to stainless steel [J]. Materials and Manufacturing Processes, 25, 2010: 1317−1323.

[18] FENG J C, LI Y L, HE P, LIU H J, YAN J C. Microstructure and strength of TiAl/steel joint induction brazed with Ag−Cu−Ti filler metal [J]. Materials Science and Technology, 2005, 21: 255−258.

[19] SHENG G M, HUANG J W, QIN B, ZHOU B, QIU S Y, LI C. An experimental investigation of phase transformation superplastic diffusion bonding of titanium alloy to stainless steel [J]. Journal of Materials Science, 2005, 40: 6385−6390.

[20] TOMASHCHUK I, SALLAMAND P, BELYAVINA N, PILLOZ M. Evolution of microstructures and mechanical properties during dissimilar electron beam welding of titanium alloy to stainless steel via copper interlayer [J]. Materials Science and Engineering A, 2013, 585: 114−122.

[21] THIRUNAVUKARASU G, KUNDU S, MISHRA B, CHATTERJEE S. Effect of bonding time on interfacial reaction and mechanical properties of diffusion-bonded joint between Ti−6Al−4V and 304 stainless steel using nickel as an intermediate material [J]. Metallurgical and Materials Transactions A, 2014, 45: 2078−2090.

[22] DEY H C, ASHFAQ M, BHADURI A K, RAO K P. Joining of titanium to 304L stainless steel by friction welding [J]. Journal of Materials Processing Technology, 2009, 209: 5862−5870.

[23] LEE W B, JUNG S B. Effect of microstructure on mechanical properties of friction-welded joints between Ti and AISI 321 stainless steel [J]. Materials Transactions, 2004, 45: 2805−2811.

[24] KUMAR R, BALASUBRAMANIAN M. Experimental investigation of Ti−6Al−4V titanium alloy and 304L stainless steel friction welded with copper interlayer [J]. Defence Technology, 2015, 11: 65−75.

[25] COBB H M. Dictionary of metals [M]. Ohio: ASM International, 2012.

[26] KAZAKOV N F. Diffusion bonding of materials [M]. Moscow: Mir Publishers, 1985.

[27] ASTM International. Annual Book of ASTM E8M-11 standard [M]. Philadelphia: ASTM, 2012.

[28] KUNDU S, CHATTERJEE S. Interfacial microstructure and mechanical properties of diffusion-bonded titanium–stainless steel joints using a nickel interlayer [J]. Materials Science and Engineering A, 2006, 425: 107−113.

[29] HINOTANI S, OHMORI Y. The microstructure of diffusion-bonded Ti/Ni interface [J]. Transactions of the Japan Institute of Metals, 1988, 29: 116−124.

[30] KUNDU S, MISHRA B, OLSON D L, CHATTERJEE S. Interfacial reactions and strength properties of diffusion bonded joints of Ti64 alloy and 17-4PH stainless steel using nickel alloy interlayer [J]. Materials and Design, 2013, 51: 714−722.

[31] KUNDU S, SAM S, CHATTERJEE S. Interfacial reactions and strength properties in dissimilar titanium alloy/Ni alloy/microduplex stainless steel diffusion bonded joints [J]. Materials Science and Engineering A, 2013, 560: 288−295.

[32] FISCHER T. Materials science for engineering students [M]. San Diego: Academic Press, 2009.

[33] PORTER D A, EASTERLING K E, SHERIF M Y. Phase transformations in metals and alloys [M]. 3rd ed. Boca Raton: CRC, 2009.

[34] MESSLER R W Jr. The essence of materials for engineers [M]. Burlington: Jones & Bartlett, 2011.

[35] THIRUNAVUKARASU G, KUNDU S, CHATTERJEE S. The latent fingerprint in mass transport of polycrystalline materials [J]. Heat and Mass Transfer, 2016, 52: 217−225.

[36] DIETER G E. Mechanical metallurgy [M]. Singapore: McGraw-Hill, 1988.

[37] SAM S, KUNDU S, CHATTERJEE S. Diffusion bonding of titanium alloy to micro-duplex stainless steel using a nickel alloy interlayer: Interface microstructure and strength properties [J]. Materials and Design, 2012, 40: 237−244.

[38] KELLY P F. Properties of materials [M]. Boca Raton: CRC, 2015.

[39] WHITE M A. Physical properties of materials [M]. Boca Raton: CRC, 2012.

[40] LOVELL M C, AVERY A J, VERNON M W. Physical properties of materials [M]. Berkshire: Van Nostrand Reinhold (U.K.), 1984.

[41] POLMEAR I J. Light alloys—From traditional alloys to nanocrystals [M]. 4th ed. Oxford: Butterworth-Heinemann, 2006.

[42] BRANDES E A, BROOK G B. Smithells metals reference book [M]. 7th ed. Oxford: Butterworth-Heinemann, 1992.

[43] JOHN V. Introduction to engineering materials [M]. 3rd ed. London: Macmillan, 1992.

[44] SIMÕES S, VIANA F, KOÇAK M, RAMOS A S, VIEIRA M T, VIEIRA M F. Diffusion bonding of TiAl using reactive Ni/Al nanolayers and Ti and Ni foils [J]. Materials Chemistry and Physics, 2011, 128: 202−207.

不锈钢/有色金属异质接头的性能优化

Gopinath THIRUNAVUKARASU, Subrata CHATTERJEE, Sukumar KUNDU

Department of Metallurgy and Materials Engineering,
Indian Institute of Engineering Science and Technology, Shibpur, Howrah 711103, India

摘　要：不锈钢/有色金属异质接头对于先进机械和传统体系设计的前沿研究具有十分重要的意义。本文作者对钛基和铁基两种异质合金进行焊接以提高异质接头的力学性能。在粘接压力范围为 1~9 MPa(步长为 2 MPa)、750 °C 和 60 min 条件下进行焊接获得异质接头。同时比较了采用不同机制和方法得到的钛基和铁基异质接头的力学性能。结果表明，扩散焊接钛、铁基异质金属接头的力学性能得到明显改善。异质金属接头优异的力学性能主要是由于在扩散区产生了能避免脆性 Fe−Ti 基金属间化合物形成的厚度约为 200 μm 的 Ni 金属第三相。所得异质接头的最大抗拉强度为 560 MPa，伸长率约为 11.9%，这是至今为止文献所报道的最佳值。当焊接压力不低于 5 MPa 时，异质接头显示出加工硬化效应。异质接头中钛基有色金属的膨胀率远高于黑色金属(不锈钢)的膨胀率。采用 SEM 技术研究反应区的详细情况，并用 XRD 验证 SEM 的结果。分析异质接头的力学、物理和断裂性能随焊接参数变化的原因。

关键词：扩散焊；钛合金；不锈钢；镍；中间层；抗拉强度；断口组织

(Edited by Wei-ping CHEN)